NASA TECHNICAL NOTE

NASA TN D-6196

NONLINEAR ACOUSTIC THEORY FOR RIGID POROUS MATERIALS

by William E. Zorumski and Tony L. Parrott

Langley Research Center
Hampton, Va. 23365

NATIONAL AERONAUTICS AND SPACE ADMINISTRATION • WASHINGTON, D. C. • JUNE 1971

1. Report No.	2. Government Accession No.	3. Recipient's Catalog No.
NASA TN D-6196		

4. Title and Subtitle	5. Report Date
NONLINEAR ACOUSTIC THEORY FOR RIGID POROUS MATERIALS	July 1971
	6. Performing Organization Code
7. Author(s)	8. Performing Organization Report No.
William E. Zorumski and Tony L. Parrott	L-7327
	10. Work Unit No.
9. Performing Organization Name and Address	126-61-14-01
NASA Langley Research Center Hampton, Va. 23365	11. Contract or Grant No.
	13. Type of Report and Period Covered
12. Sponsoring Agency Name and Address	Technical Note
National Aeronautics and Space Administration Washington, D.C. 20546	14. Sponsoring Agency Code

15. Supplementary Notes

16. Abstract

Nonlinear instantaneous relationships between acoustic pressure differential and velocity are postulated to describe the acoustic characteristics of a rigid porous material, and the concept of a temporal impedance operator is introduced. The new theory is valid for any wave, irrespective of frequency, intensity, or distortion. A new experimental method is given for measuring these properties in a high-intensity impedance tube. The measurement method is independent of wave distortion. Results of an experimental study of a typical material are presented in terms of nonlinear instantaneous resistance and reactance. The instantaneous resistance is found to be independent of the test frequency and is therefore identical to the flow resistance. The instantaneous reactance is found to be a function of the acoustic fluid velocity.

17. Key Words (Suggested by Author(s))	18. Distribution Statement
Nonlinear acoustic impedance Acoustic materials	Unclassified – Unlimited

19. Security Classif. (of this report)	20. Security Classif. (of this page)	21. No. of Pages	22. Price*
Unclassified	Unclassified	26	$3.00

*For sale by the National Technical Information Service, Springfield, Virginia 22151

NONLINEAR ACOUSTIC THEORY FOR RIGID POROUS MATERIALS

By William E. Zorumski and Tony L. Parrott
Langley Research Center

SUMMARY

Nonlinear instantaneous relationships between acoustic pressure differential and velocity are postulated to describe the acoustic characteristics of a rigid porous material, and the concept of a temporal impedance operator is introduced. The new theory is valid for any wave, irrespective of frequency, intensity, or distortion. A new experimental method is given for measuring these properties in a high-intensity impedance tube. The measurement method is independent of wave distortion. Results of an experimental study of a typical material are presented in terms of nonlinear instantaneous resistance and reactance. The instantaneous resistance is found to be independent of the test frequency and is therefore identical to the flow resistance. The instantaneous reactance is found to be a function of the acoustic fluid velocity.

INTRODUCTION

Previous studies of nonlinear acoustic effects in porous materials have been made by using the assumption of nearly simple harmonic motion. In reference 1, Sivian studied the acoustic resistance and reactance of an orifice and found that reactance did not depend strongly on velocity amplitude, but that resistance increased with amplitude for large velocities. A study by Bolt, Labate, and Ingard (ref. 2) showed that the reactance should decrease with particle velocity, and confirmed Sivian's increasing resistance effect. They also found that the reactance was proportional to the frequency. Further theoretical and experimental work on orifices and resonators was done by Ingard (ref. 3), Bies and Wilson (ref. 4), and Thurston, Hargrove, and Cook (ref. 5). The authors of reference 5 were the first to consider the coupling between a steady flow and oscillating flow in an orifice. They noted that a sinusoidal flow caused added higher odd harmonics and that the superposition of a steady flow caused added even and odd harmonics of the fundamental frequency. In a more recent paper, Ingard and Ising (ref. 6) studied the nonlinearity of an orifice by measuring the amplitudes and relative phase of pressure and particle velocity at the orifice. They also noted the higher harmonics and carried out a study of the effect of a superimposed steady flow on the impedance of the fundamental wave.

In an attempt to give a simple empirical explanation of the nonlinear phenomena observed in perforated plates and porous materials, a pair of simultaneous relations was proposed in reference 7. The first was that the instantaneous normal particle velocity should be equal on opposite sides of a thin porous sheet. The second was that the instantaneous acoustic pressure differential was equal to the steady-flow pressure differential. These relations are time-domain characterizations of the material, as opposed to the usual spectral impedance method of description, which is an averaged frequency-domain characterization. In reference 7, the steady-flow resistance of a typical material was measured and used to predict the impedance of the material. Experimental measurements showed a fair correspondence between predicted and acoustically measured resistance. The acoustic measurements also revealed a small, nearly constant reactive component of impedance. These simple ideas were generalized into a set of general empirical laws governing the instantaneous flux of mass, momentum, and energy through a thin porous sheet. (See ref. 8.) These laws contain functions of the flow variables which must be measured.

In the present paper, it is postulated that an acoustic material may be empirically described by two nonlinear functions of the acoustic particle velocity. This is an extension of the theory presented in reference 7, which assumed only one nonlinear function. The new theory is a special case of the general laws presented in reference 8.

Since the nonlinear functions depend only on particle velocity, the theory is invariant with respect to distortion of the wave. Spectral impedance representations are difficult to obtain in the high-intensity region because coupling between different frequency waves makes the spectral impedance depend on wave distortion. A high-intensity impedance tube measurement (by the standard method) depends on the properties of the tube as well as on the properties of the material. A method of measuring the nonlinear function is given in this paper. The measurement method, like the new theory, is invariant with respect to wave distortion so that the properties of the impedance tube should not affect the measured nonlinear functions.

An experimental program was designed to verify the theoretical model of material behavior. Tests were made at standard fundamental frequencies of 500, 1000, 2000, and 4000 Hz. These tests were used to investigate the possibility of any explicit dependence of the nonlinear functions on frequency. At each frequency, the intensity was varied from about 120 dB to the highest attainable level. The variation in intensity was used to investigate the dependence of the nonlinear functions of particle velocity over a range from about 3.5 cm/sec up to about 350 cm/sec. Measured data from each test were compared with data calculated from the theory of reference 7, and the measured data were reduced to obtain the nonlinear functions in the new theory.

SYMBOLS

When symbols represent dimensionless groups, the definition is given in the form of an equation.

c speed of sound, meters per second (m/s)

f frequency, hertz (Hz)

f_r reference frequency, hertz (Hz)

L_1, L_2 undetermined momentum functions

M_1, M_2 undetermined mass functions

n denotes harmonic number ($n = 1$ is the fundamental)

$$p = \frac{\text{Pressure}}{\rho c^2}$$

$$p_n = \frac{\text{Complex pressure amplitude}}{\rho c^2}$$

$$q = \frac{\text{Acoustic velocity}}{c}$$

$$q_n = \frac{\text{Complex velocity amplitude}}{c}$$

$$R = \frac{\text{Acoustic resistance}}{\rho c}$$

$$R[V] = \frac{\text{Acoustic resistance as a function of } V}{\rho c}$$

$$R_n = \frac{\text{Spectral resistance}}{\rho c}$$

$$t = \omega \times \text{Time}$$

$$V = \frac{\text{Velocity through material}}{c}$$

$$V_n = \frac{\text{Complex amplitude of velocity through material}}{c}$$

$$x = \frac{2\pi \times \text{Distance from material}}{\lambda}$$

$X = \frac{\text{Acoustic reactance}}{\rho c}$

$X[V] = \frac{\text{Acoustic reactance as a function of } V}{\rho c}$

$X_n = \frac{\text{Spectral reactance}}{\rho c}$

$Z_n = \frac{\text{Spectral impedance}}{\rho c}$ or $Z_n = R_n - iX_n$

$Z_t = \frac{\text{Temporal impedance operator}}{\rho c}$ or $Z_t = R[V] + X[V]\frac{\partial}{\partial t}$

δ material thickness, meters (m)

$\Delta[\,]$ denotes differential in variable enclosed in brackets

λ wavelength, meters (m)

ρ density, kilograms per cubic meter (kg/m^3)

ω circular frequency, radians per second (rad/s)

ANALYSIS

Material Properties

Figure 1 shows an element of a sheet of porous material which is enclosed by a control volume. In general, the pressure, density, and flow velocity are different on

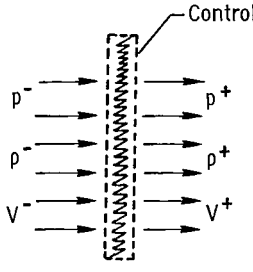

Conservation of mass

$$\Delta[\rho V] = \frac{\partial M_1}{\partial t} + M_2$$

Conservation of momentum

$$\Delta[p] = \frac{\partial L_1}{\partial t} + L_2$$

Figure 1.- Mass and momentum flux through sheet of rigid porous material.

opposite sides of the porous sheet. Applying the principle of conservation of mass to the control volume gives

$$\Delta[\rho V] = \frac{\partial M_1}{\partial t} + M_2 \tag{1}$$

The left-hand side of equation (1) represents the difference between the inflow of mass on one side of the sheet and the outflow on the other side. The time derivative of the function M_1 represents the rate at which mass is stored within the control volume. The function M_2 is introduced to account for jetting effects. Similarly, application of the principle of conservation of momentum yields

$$\Delta[p] = \frac{\partial L_1}{\partial t} + L_2 \tag{2}$$

A thorough derivation of equations (1) and (2) is given in reference 8.

In equations (1) and (2), the symbol Δ may be regarded as the discontinuity, in the bracketed variables, at a sheet of material with negligible thickness. The functions M_1, M_2, L_1, and L_2 depend on the acoustic variables and on the material. These functions must be determined experimentally and their measurements must be made in the time domain. For the first-order approximation, the left-hand side of equation (1) represents the velocity discontinuity at a thin porous sheet of material. The functions M_1 and M_2 may take on appreciable values only if there are significant compressibility effects within the porous material and severe variations in the distribution of velocity and density over the material surface due to jetting effects. These will be assumed to be negligible so that equation (1) is satisfied, to the first approximation, by having the acoustic velocity continuous across the porous sheet.

In a steady flow, the time-derivative term in equation (2) drops out; therefore, the function L_2 can be determined by measuring the pressure differential across the porous material in a steady flow test. It has been shown (refs. 9 and 10) that this function can be given, as suggested by dimensional analysis, in terms of Reynolds number and Mach number. For any given material, with the small pressure and density perturbations of acoustics, the Reynolds number and Mach number vary primarily with the velocity. Thus, the function L_2 is, in the first-order approximation, a function of velocity only and may be given as

$$L_2 = R[V]V \tag{3}$$

where $R[V]$ is the acoustic resistance function. Consequently, for thin porous sheets of material, the material may be represented by the equations

$$\Delta[V] = 0 \tag{4a}$$

$$\Delta[p] = \frac{\partial L_1}{\partial t} + R[V]V \tag{4b}$$

The problem of characterizing a material is now reduced to determining the function $\frac{\partial L_1}{\partial t}$. If $R[V]$ is measured, then equation (4b) gives this function for the wave used in the measurement. In order to find this function for any wave, it is necessary to determine its general form. For this study, it will be assumed that

$$\frac{\partial L_1}{\partial t} = X[V]\frac{\partial V}{\partial t} \tag{5}$$

This equation is the simplest nonlinear form for L_1. Equation (5) is suggested by the results of low-intensity measurements. For values of V sufficiently small, $R[V]$ and $X[V]$ approach constants, and, for harmonic time variation e^{-int}, the operator $\partial/\partial t$ may be replaced by $(-in)$ so that for the nth harmonic

$$\Delta[p_n] = (R - inX)V = Z_n V_n \tag{6}$$

where Z_n is the spectral impedance of the nth harmonic. Measurements indicate that the low-intensity resistance is equal to the flow resistance. The acoustic reactance X is found to be a small positive constant at low intensities and may be interpreted as the effective mass of the gas within the porous material.

Combining equations (4) and (5) gives

$$\Delta[p(t)] = \left(R[V(t)] + X[V(t)]\frac{\partial}{\partial t}\right)V(t) = Z_t V(t) \tag{7}$$

where Z_t is defined as the temporal impedance operator. It is impossible to derive rigorously the expression for the temporal impedance operator Z_t. Therefore, its existence should be regarded as a basic postulate to be verified by experimental studies.

The functions $X[V]$ and $R[V]$ may be found from a parametric plot of $\Delta[p(t)]$ against $V(t)$. Figure 2 shows a typical trajectory of this type for a periodic disturbance. On this trajectory, a point $(V, \Delta[p])$ moves, with increasing time, in the direction indicated by arrows in figure 2 and describes a closed circuit about the origin. If two points on the trajectory (for example, t_1 and t_2) are chosen so that the velocities are equal at these times, then

$$\begin{bmatrix} V(t_1) & \frac{\partial V(t_1)}{\partial t} \\ V(t_2) & \frac{\partial V(t_2)}{\partial t} \end{bmatrix} \begin{Bmatrix} R[V] \\ X[V] \end{Bmatrix} = \begin{Bmatrix} \Delta[p(t_1)] \\ \Delta[p(t_2)] \end{Bmatrix} \tag{8}$$

Equation (8) may be inverted to find the unknown functions. Varying t_1, and thus $V(t_1)$, then gives the desired functions of velocity. Assuming a nearly harmonic motion, the solution to equation (8) shows that the reactance is roughly proportional to the vertical distance from point 2 to point 1. (See fig. 2.) The resistance is proportional to the distance between points 3 and 4.

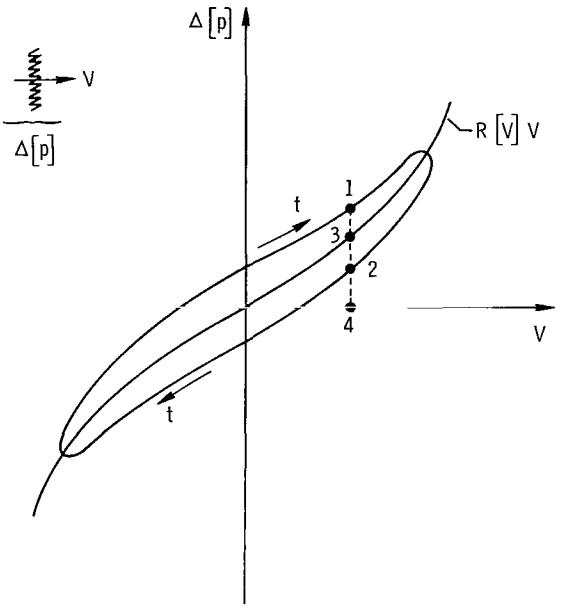

Figure 2. - Typical trajectory of instantaneous pressure differential and velocity for thin porous material.

For low-intensity sound, the same constants, R and X, appear in both types of impedance. For high-amplitude sound waves, it has been shown that the spectral impedance is related to amplitude as well as to frequency and that the spectral impedance at a given frequency (refs. 5 and 6) may be modified by the addition of a small steady flow (zero frequency). Therefore, the spectral impedance at one frequency can be affected by a sound at another frequency. For a distorted periodic wave, the spectral impedance of a material (at high intensities) will depend in some manner upon all velocity harmonics at the sample. In general, a material could be completely characterized by a spectral

impedance relation of the form

$$\Delta\left[p_n\right] = Z_n\left(V_0, V_1, V_2, \ldots\right)V_n,\ n = 0,1,2, \ldots \tag{9}$$

In references 5 and 6, the dependence of Z_1 upon V_0 and V_1 was studied. There has been no previous investigation of the general relationship in equation (9). It is apparent that the direct experimental measurement of nonlinear spectral impedance is a formidable task. Unless some form of the function $Z_n\left(V_0, V_1, V_2, \ldots\right)$ is known, it would have to be measured for all possible combinations of the velocity harmonics. It is of interest to note that there is a functional relationship between the temporal impedance in equation (7) and the spectral impedance in equation (9). This relationship may be obtained by substituting Fourier series for the temporal variables $\Delta\left[p(t)\right]$ and $V(t)$ in equation (7). Therefore, if the temporal impedance is known, the spectral impedance may be calculated for any intensity, frequency, and combination of harmonics.

Basis of Measurement Method

In order to study the nonlinear acoustic properties of materials in the high-intensity region, it is necessary to make measurements of a curve such as the one shown in figure 2. The results of these measurements may be given in terms of the acoustic impedance of the material or in terms of some instantaneous relation between pressure and velocity. At low acoustic intensities, where the sound is a simple harmonic wave, these descriptions are simply related. At high intensities, their relationship is much more complex.

Figure 3 shows the device which is used to determine $\Delta p(t)$ and $V(t)$. A signal is provided by the speaker. Because of nonlinearities in the air, in the sample, and in the speaker, the signal will become distorted at high amplitudes. Pressures are measured by microphones placed in front of and behind the sample.

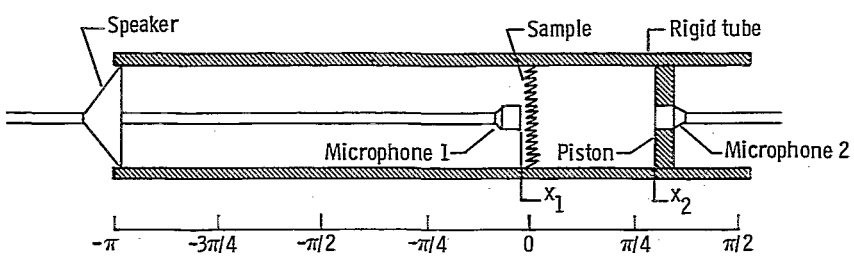

Figure 3. - Impedance tube.

The following analysis presents the necessary theoretical basis for reducing the pressure measurements to the desired time histories of $\Delta[p(t)]$ and $V(t)$.

If the microphones are placed near the sample, it is permissible to use the linear one-dimensional wave equation:

$$\frac{\partial^2 p}{\partial x^2} = \frac{\partial^2 p}{\partial t^2} \tag{10}$$

The acoustic velocity is related to the pressure by

$$\frac{\partial q}{\partial t} = - \frac{\partial p}{\partial x} \tag{11}$$

Periodic solutions to equation (10) which also satisfy equation (11) are

$$q = \sum_{n=-\infty}^{\infty} \left(u_n e^{inx} + v_n e^{inx}\right) e^{-int} \tag{12}$$

and

$$p = \sum_{n=-\infty}^{\infty} \left(u_n e^{inx} - v_n e^{-inx}\right) e^{-int} \tag{13}$$

where u_n and v_n are the complex velocity amplitudes of right-moving and left-moving waves, respectively. The terms in parentheses in equations (12) and (13) are the complex velocity and pressure amplitude at the point x; that is,

$$q_n(x) = u_n e^{inx} + v_n e^{-inx} \tag{14}$$

and

$$p_n(x) = u_n e^{inx} - v_n e^{-inx} \tag{15}$$

Throughout the discussion, it is understood that complex coefficients with negative subscripts are the conjugate of those with positive subscripts. For example, $u_n = \left(\overline{u_{-n}}\right)$. This satisfies the condition that the physical quantities are represented by real variables.

The complex spectral impedance is defined to be

$$Z_n(x) = \frac{p_n(x)}{q_n(x)} \tag{16}$$

Consider the impedance tube shown schematically in figure 3. It is desired to use this device to measure the complex impedance of the sample of porous material. This impedance is

$$Z_n = Z_n^{(-)} - Z_n^{(+)} \tag{17}$$

where superscripts (+) and (-) indicate front and back of the sample, respectively. If the velocity is assumed to be continuous through the sample,

$$q_n^{(-)} = q_n^{(+)} = V_n \tag{18}$$

the spectral impedance is given by

$$Z_n = \frac{\Delta[p_n]}{V_n} \tag{19}$$

where

$$\Delta[p_n] = p_n^{(-)} - p_n^{(+)} \tag{20}$$

Two complex pressure measurements are required to find the material impedance. If a small microphone is placed in a rigid wall at x_2 (see fig. 3), then

$$p_n^{(+)} = p_n(x_2) \cos(nx_2) \tag{21}$$

$$V_n = -ip_n(x_2) \sin(nx_2) \tag{22}$$

and

$$p_n^{(-)} = \frac{p_n(x_1)}{\cos(nx_1)} - \tan(nx_1) \sin(nx_2)\, p_n(x_2) \tag{23}$$

Since the time base is arbitrary, the phase angle of the fundamental at one microphone may be set to zero. The phase angles of higher harmonics at that microphone must be determined through Fourier analysis of the signal. The amplitudes of all harmonics may be measured directly or may be found from Fourier analysis. It is therefore theoretically possible to measure the spectral impedances of each harmonic of a distorted wave by using two microphones in a traveling wave tube. Note that the method given here is considerably more involved than the standard method of impedance measurement described in reference 11. However, the standard method can only be used to measure the spectral impedance of a pure harmonic wave. The present method may be used to measure nonlinear spectral impedance of distorted waves.

Measurements of the complex pressure harmonics may also be used to find the instantaneous values of pressure differential and velocity. They are given by

$$\Delta[p(t)] = \sum_{n=-\infty}^{\infty} \Delta[p_n] e^{-int} \tag{24}$$

$$V(t) = \sum_{n=-\infty}^{\infty} V_n e^{-int} \tag{25}$$

The temporal impedance functions may be found by using these equations with equation (8).

EXPERIMENTS

Preliminary Tests

Before the main test series began, a qualitative study of the instantaneous relationship between pressure differential and velocity was made for the material sample. The rigid piston shown in figure 3 was removed and replaced by a ρc (nonreflecting) termination. Since both microphones were placed very near the sample, the difference in their signals was a measure of pressure differential, and the signal of microphone 2 was proportional to the velocity through the material. The pressure differential $\Delta[p]$ was displayed on the vertical axis and the velocity was used to sweep the horizontal axis of an oscilloscope so that a trajectory, like the one shown in figure 2, could be photographed.

A test was made at a frequency of 1000 Hz. At low intensity, the trajectory was an ellipse, as predicted by linear theory. As the intensity was increased, the trajectory began to distort as shown in figure 2; however, at the highest intensities which could be reached, a trajectory with loops on the ends was formed. (See fig. 4.) These loops show

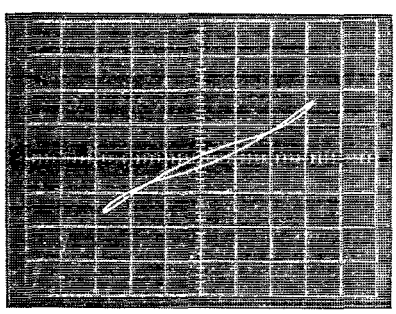

Figure 4.- Oscilloscope display of pressure differential as a function of velocity. f = 1000 Hz; SPL = 155 dB.

that the nonlinear reactance $X[V]$ in equation (8) becomes negative at large velocities. Since $X[V]$ depends approximately on the difference between the upper and lower curves, such as between points 1 and 2 shown in figure 2, then, when these curves cross, there may be a change in sign of the reactance. Equation (8) must be solved to determine if the reactance actually does become negative.

Attempts to measure quantitatively the pressure-velocity trajectories by using the ρc termination gave poor results. This was believed to be primarily due to the small pressure drop across the sample which resulted in loss of accuracy when the signals were subtracted. To alleviate this problem, the rigid piston shown in figure 3 was installed and set at 1/4 wavelength ($\lambda/4$) from the sample to give a pressure null behind the sample for the odd harmonics. This arrangement was used in the main test program.

Preliminary studies were made of the flow resistance of three different samples: a perforated plate, a porous metallic sample, and a fiber-glass—plastic sample. The fiber-glass—plastic sample had the most nonlinear flow resistance and was chosen for the main test program.

Instrumentation

A block diagram of the instrumentation is shown in figure 5. The fundamental frequency is generated by the frequency synthesizer, which provides an accurate and drift-free signal. Output from the synthesizer goes to the power amplifier which drives the

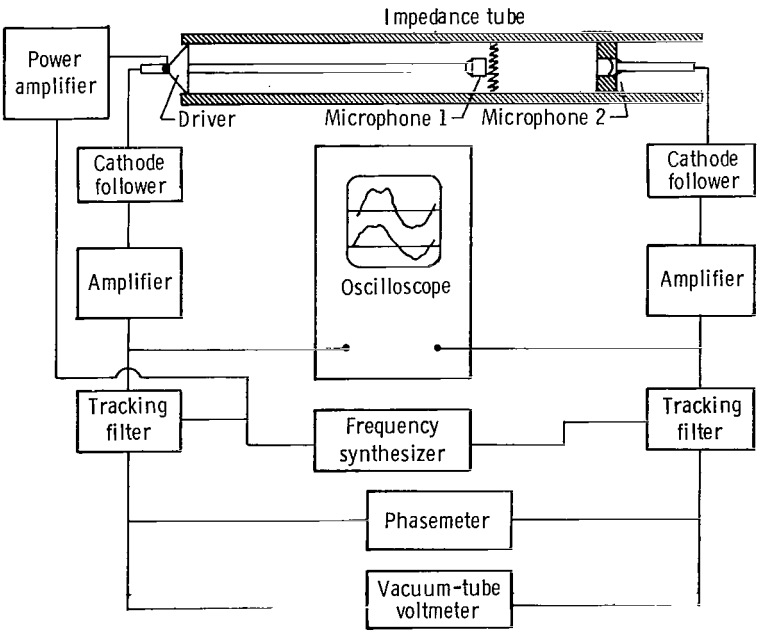

Figure 5. - Block diagram of instrumentation.

sound source in the impedance tube. The synthesizer also provides a center frequency reference for the tracking filters. The signals from each microphone—cathode follower were amplified and displayed on a dual-channel oscilloscope. Amplifier outputs were also sent to the tracking filters which removed all distortion from the signals. Relative phase of the fundamental signal output from the tracking filters was monitored by the phasemeter. Amplitude of these signals were measured by an rms voltmeter.

Calibration Procedure

It was verified that the transducers and electronic equipment had linear amplitude frequency response. The phase shift is also assumed to be a linear function of frequency. The linear phase shift produces no distortion of the signals, but it does produce a shift in the time base; therefore, the voltage observed on the oscilloscope is not in phase with the pressure at the transducer face. Since the two channels were not phase-matched, it was necessary to compensate for the difference in time base of the two signals displayed on the oscilloscope as follows:

With the sample removed, the microphones are pushed together and excited at the test frequency. The reading on the phasemeter was noted and the phase difference between the fundamental pressure harmonics could be determined from a second phasemeter reading during the test run. The tracking filters insured a harmonic signal at the phasemeter; therefore, its accuracy was not impaired by the distortion of the pressure signal. The signals displayed on the oscilloscope were Fourier analyzed with respect to a common time base. The phase difference between the fundamental voltage harmonics could then be determined from the complex Fourier coefficients. A comparison of the fundamental voltage phase difference with the fundamental pressure phase difference gave the desired phase calibration between the pressure and voltage signals.

Amplitude calibration of the system was made at 250 Hz with the use of a pistonphone which produced a 124-dB reference. The voltmeter reading for this reference pressure was noted. At the test frequency, the microphones were placed together and the second channel was amplitude adjusted to give the same voltage reading as the reference channel. The voltmeter readings could then be used to determine the fundamental pressure amplitudes for both channels during the test. With the phases and amplitudes of the fundamental pressure signals of both channels known, the complex Fourier coefficients of the higher harmonics could be determined from the Fourier analysis of the voltage signals.

Main Test Program

The main test program was planned with three objectives. The first was to examine more closely the accuracy of the theory presented in reference 7, which is that the instantaneous resistance $R[V]$ is the same as the flow resistance and that the instantaneous

reactance $X[V]$ is a constant which may therefore be measured by low-intensity tests. The second objective was to establish the validity of equation (7); that is, to show by use of dynamic tests that the instantaneous nonlinear resistance and reactance are functions (in time) of only the fluid velocity through the material. The third objective was to measure the functions $R[V]$ and $X[V]$ for a typical rigid porous material.

The dimensionless flow resistance of the sample material is shown in figure 6. For very low frequencies, this curve completely characterizes the acoustic properties of the material since the time derivative in equation (7) is negligible. The resistance curve has a small slope even at the lowest measured velocity of 2.25×10^{-4}; therefore, it is not certain whether the material has a linear range. For sound pressure levels (SPL) greater than 120 dB, however, the dimensionless velocity V should be of the order of 10^{-4} or larger so that the lowest measured resistance can be used as an approximation to the resistance for smaller velocities.

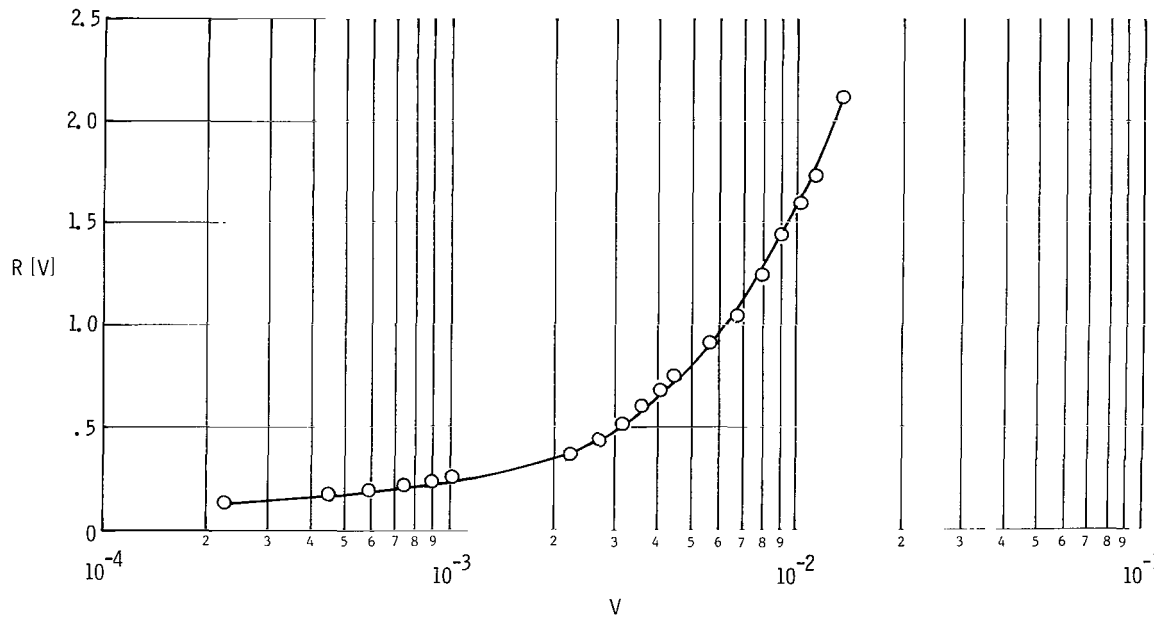

Figure 6. - Flow resistance of sample material.

The postulate of this paper is that the temporal resistance and reactance are functions of only the acoustic velocity. Therefore, these functions must be independent of the frequency of the test which is made to measure them.

Tests were made at frequencies of 500, 1000, 2000, and 4000 Hz. At each frequency the SPL in front of the sample was varied in roughly 6-dB steps from about 120 dB to the maximum level which could be obtained. At the lower frequencies, this maximum level was about 160 dB and decreased to about 150 dB at 4000 Hz. The impedance tube tended to resonate at 1800 Hz, and the measured spectral impedance of the fundamental was noted to vary erratically with both SPL and frequency when the frequency was near resonance.

RESULTS AND DISCUSSION

Sample Measurements

Photographs of the oscilloscope traces are shown in figure 7. For the lower intensities, the pressures at 500 and 4000 Hz are nearly sinusoidal (figs. 7(a) and 7(c)). At 2000 Hz, near the resonance of the impedance tube, the signals are distorted by higher harmonics. The high SPL signals shown in figures 7(d) and 7(f) are distorted due to nonlinear effects within the impedance tube. The most distortion occurs at the high-intensity

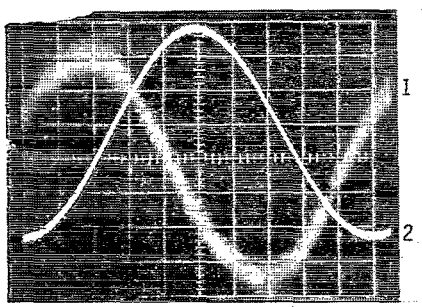

(a) f = 500 Hz; SPL = 123 dB.

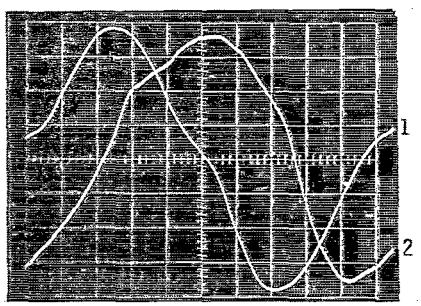

(d) f = 500 Hz; SPL = 158 dB.

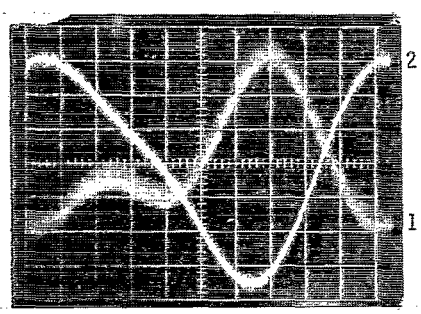

(b) f = 2000 Hz; SPL = 119 dB.

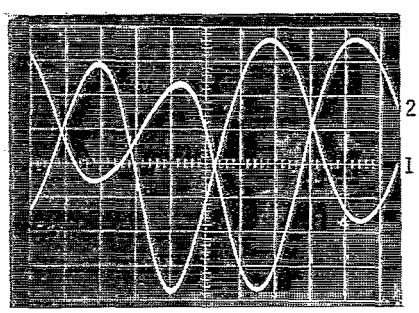

(e) f = 2000 Hz; SPL = 143 dB.

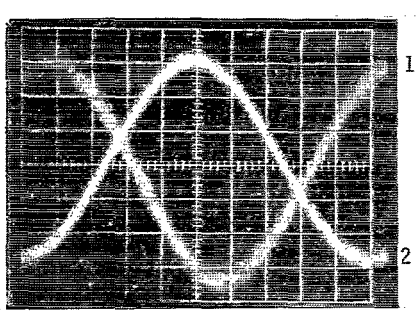

(c) f = 4000 Hz; SPL = 115 dB.

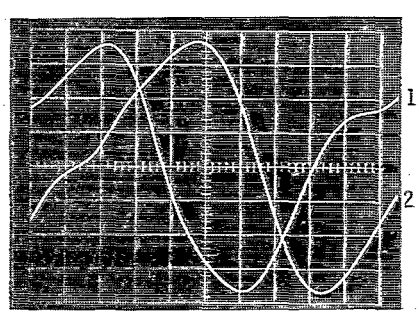

(f) f = 4000 Hz; SPL = 149 dB.

Figure 7.- Photographs of oscilloscope display of pressure signals. Channel 1 – pressure in front of sample; channel 2 – pressure on rigid piston set at $\lambda/4$ behind sample.

test at 2000 Hz, where tube resonance and material nonlinearity combine to distort the waves. These signals are typical of the ones recorded during the test program. Spectra for these signals were found by reading 50 evenly spaced points from each trace and using discrete Fourier analysis. The complex Fourier coefficients of the signal from channel 1 were corrected by the phasemeter reading, and the amplitudes of the coefficients from each channel were adjusted to conform with the pressures derived from the voltmeter readings. This procedure gave the line spectra for the dimensionless pressures, both of which were referred to a common time base. Equations (21), (22), and (23) were then used to obtain the pressure-differential and velocity spectra, $\Delta[p_n]$ and V_n. From these, the instantaneous dimensionless pressure differential $\Delta[p(t)]$ and velocity $V(t)$, were constructed from equations (24) and (25).

The measured time histories of velocity and pressure differential are shown in figures 8 to 11. The pressure differentials were also computed according to the theory of reference 7, by using equation (7) with $R[V]$ given by the measured flow resistance of figure 6 and $X[V] = f \times 10^{-4}\ \mathrm{Hz}^{-1}$. Figure 8(a) shows the measured velocity for a low-intensity test at 500 Hz. The velocity is essentially sinusoidal for this test. The measured and computed pressure differentials (fig. 8(b)) are in good agreement. Figure 8(c) shows the trajectories of pressure differential as a function of velocity. These trajectories are elliptical, since the pressure differentials are sinusoidal. As time increases, points on the trajectories move about the origin in a clockwise sense.

Data from a high-intensity test is shown in the right-hand side of figure 8. The velocity time history in figure 8(d) has noticeable distortion due to higher harmonics. In all tests, the even harmonics have been removed, since they cannot theoretically contribute to the velocity at the sample and, therefore, should not affect the pressure differential. The distortion in figure 8(d) is thus due to odd harmonics only. Odd harmonics up to the seventh were used in all tests to represent velocity and pressure differential. The measured and computed high-intensity pressure differentials (fig. 8(e)) show larger differences than the low-intensity test. Most of this difference can be accounted for by the nonlinearity in the reactive term, which can only be measured by a dynamic test. Note that the computed pressure differentials are based on a constant reactance. The computed pressure-velocity trajectory (fig. 8(f)) has the form of an elongated ellipse whose major axis is bent in the shape of the flow resistance curve. Points on this curve still move about the origin in a clockwise sense. The measured trajectory, however, has large loops on opposite ends (cf. fig. 3). Since these loops extend from near the origin to the point of maximum velocity, the reactance is negative during most of the cycle.

The general qualities of the test data at 1000 Hz (fig. 9) are the same as the data from the 500-Hz test. It may be seen from figure 9(f), however, that the reactance is positive for a larger portion of the cycle. The loops which indicate negative reactance begin at a velocity of about 5×10^{-3}, which is roughly 1/2 of the peak velocity.

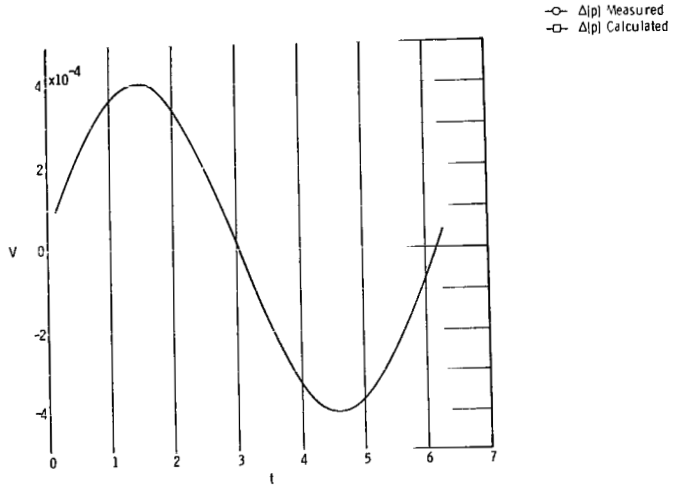

(a) Velocity. SPL = 123 db.

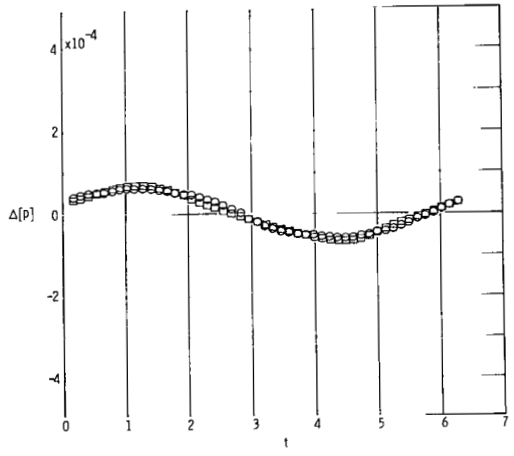

(b) Pressure. SPL = 123 db.

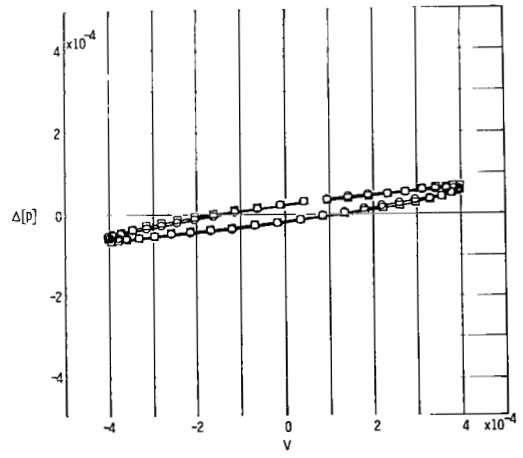

(c) Pressure - velocity trajectory. SPL = 123 db.

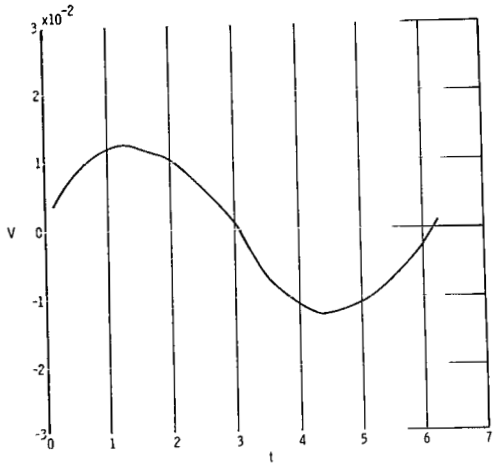

(d) Velocity. SPL = 159 db.

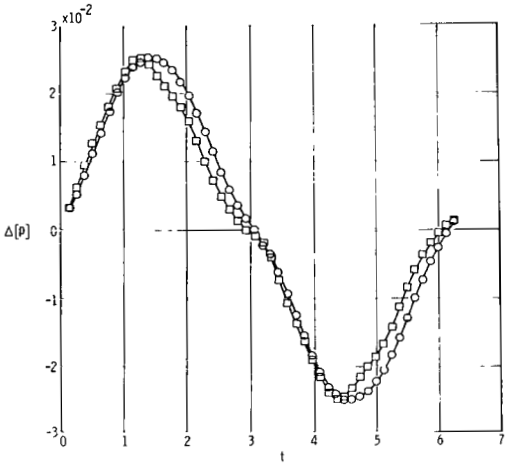

(e) Pressure. SPL = 159 db.

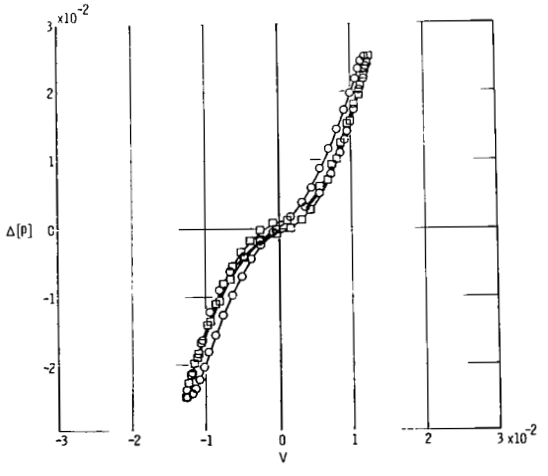

(f) Pressure - velocity trajectory. SPL = 159 db.

Figure 8.- Velocities and pressure differentials. f = 500 Hz.

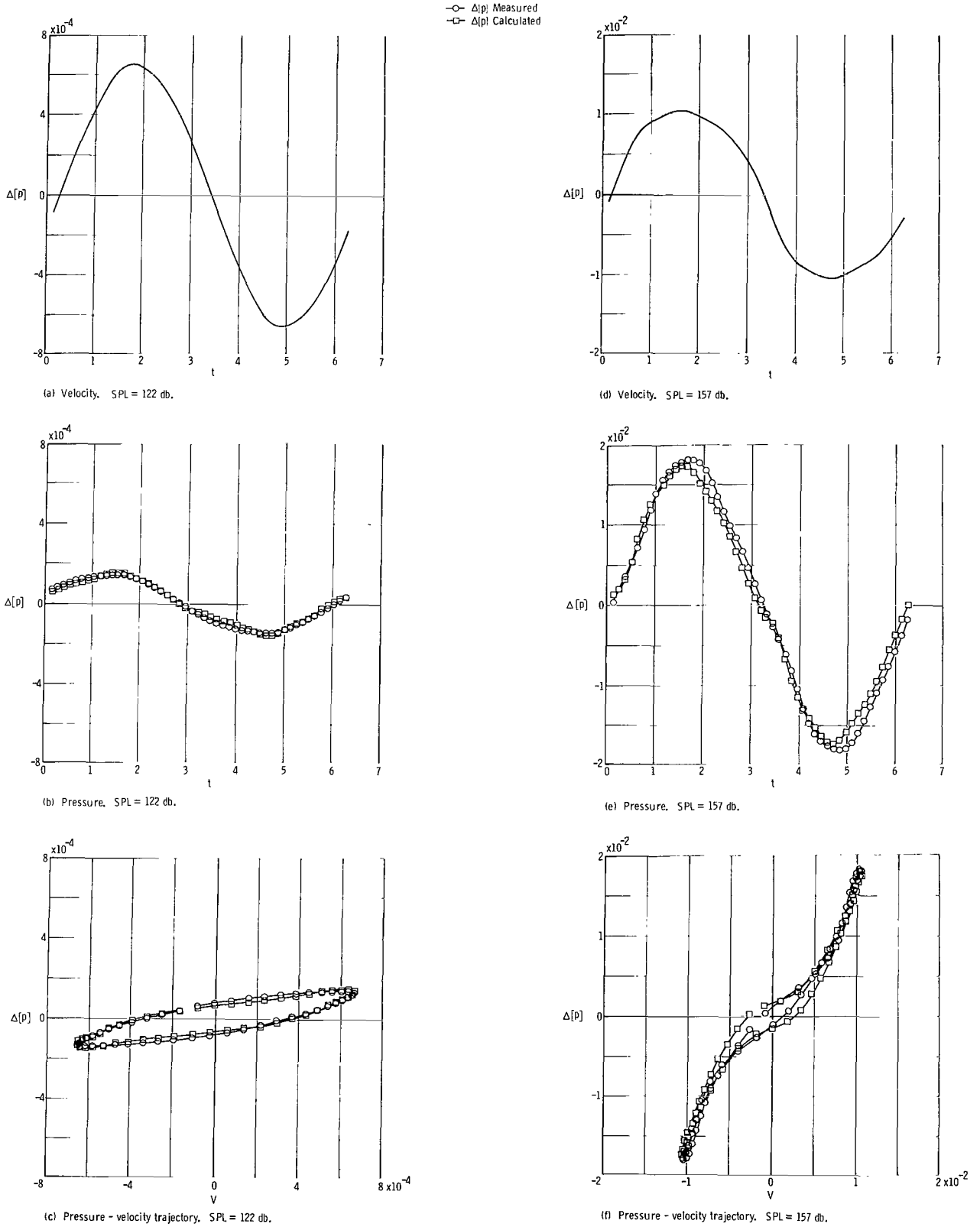

(a) Velocity. SPL = 122 db.

(b) Pressure. SPL = 122 db.

(c) Pressure - velocity trajectory. SPL = 122 db.

(d) Velocity. SPL = 157 db.

(e) Pressure. SPL = 157 db.

(f) Pressure - velocity trajectory. SPL = 157 db.

Figure 9.- Velocities and pressure differentials. f = 1000 Hz.

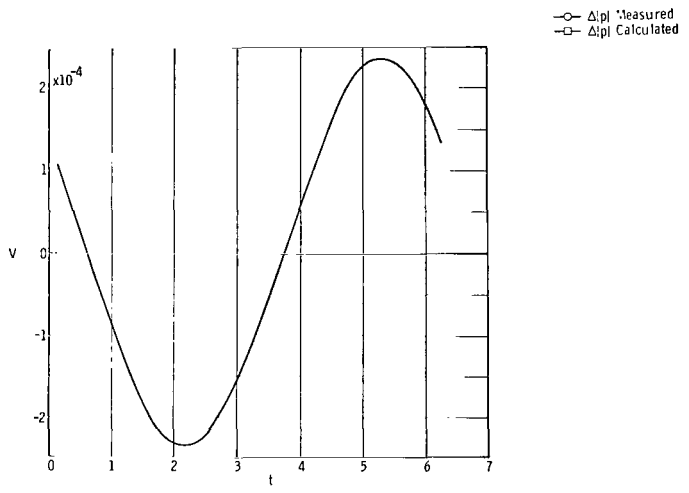

(a) Velocity. SPL = 119 db.

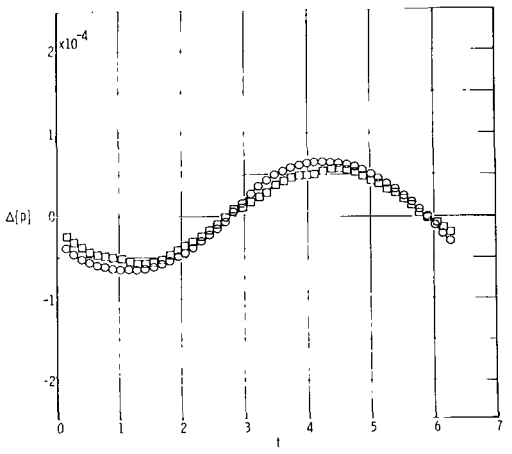

(b) Pressure. SPL = 119 db.

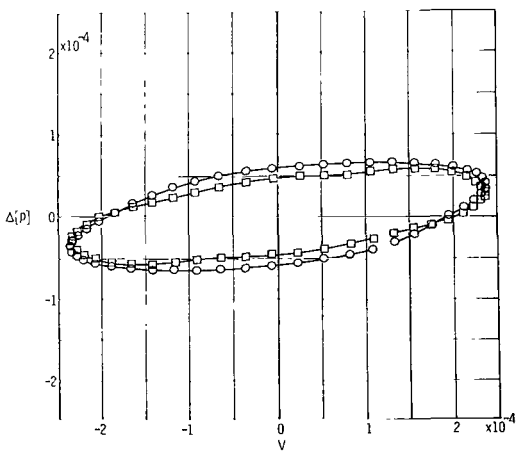

(c) Pressure -velocity trajectory. SPL = 119 db.

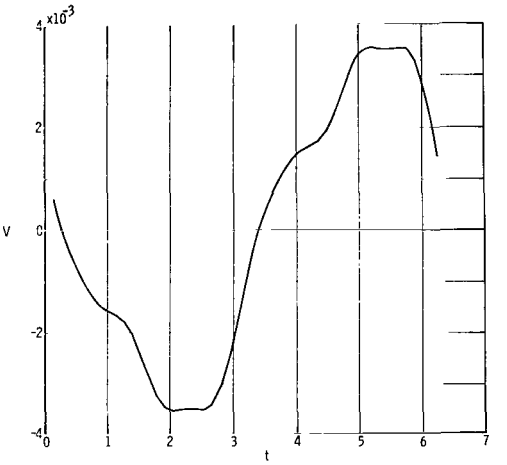

(d) Velocity. SPL = 143 db.

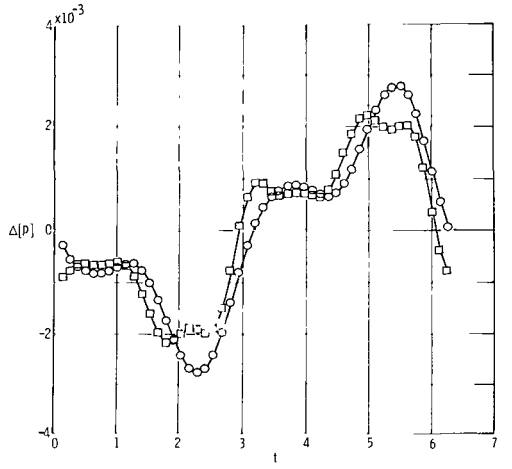

(e) Pressure. SPL = 143 db.

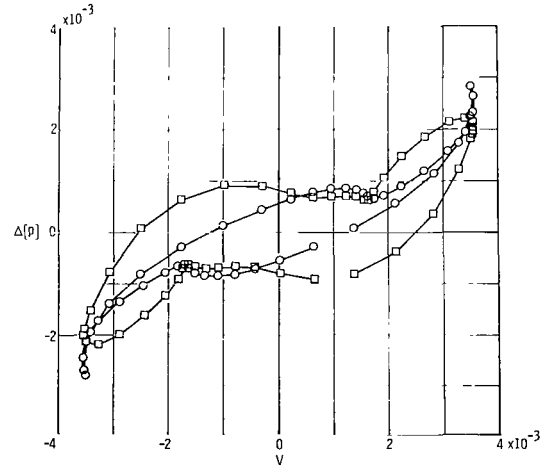

(f) Pressure - velocity trajectory. SPL = 143 db.

Figure 10.- Velocities and pressure differentials. f = 2000 Hz.

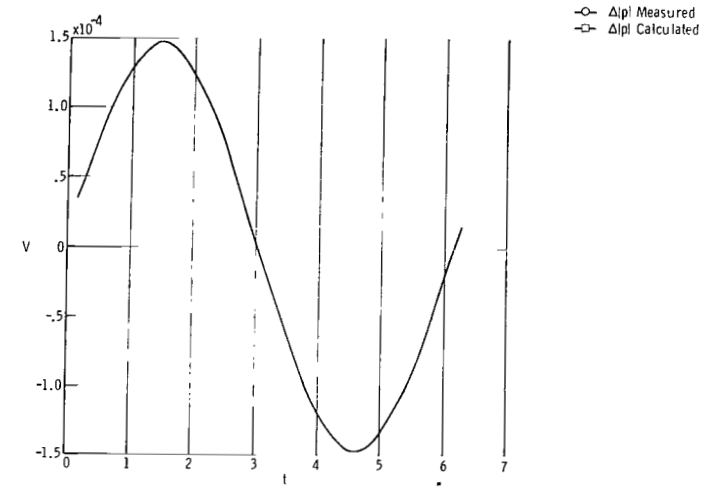

(a) Velocity. SPL = 115 db.

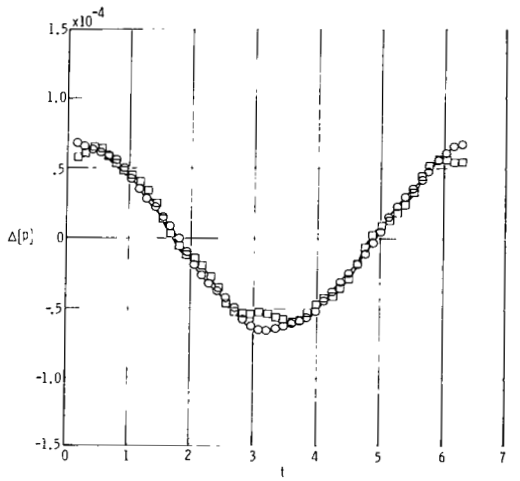

(b) Pressure. SPL = 115 db.

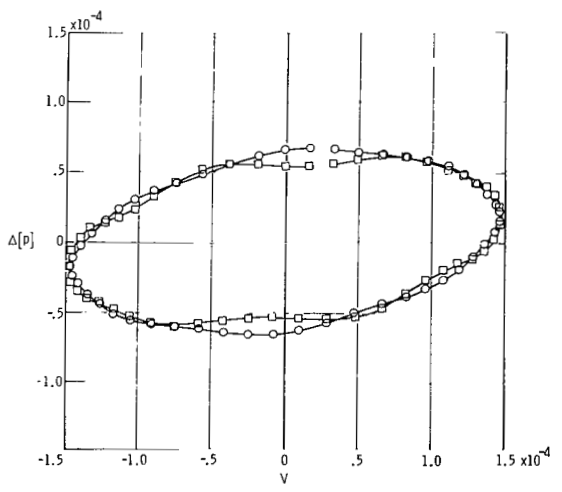

(c) Pressure - velocity trajectory. SPL = 115 db.

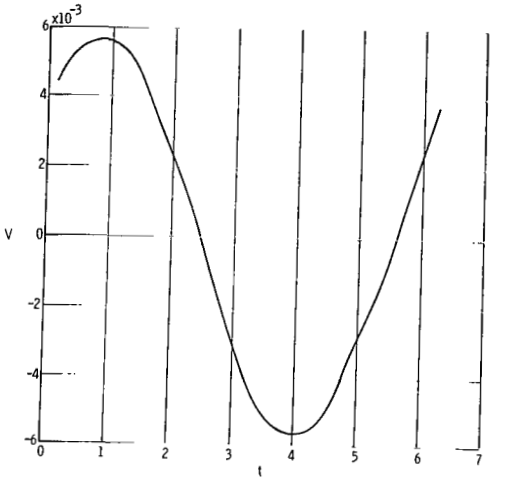

(d) Velocity. SPL = 149 db.

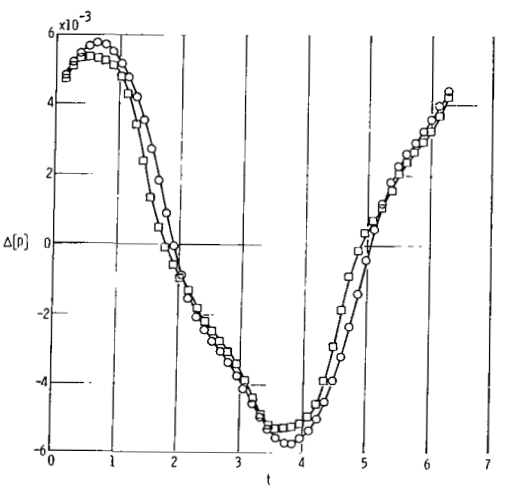

(e) Pressure. SPL = 149 db.

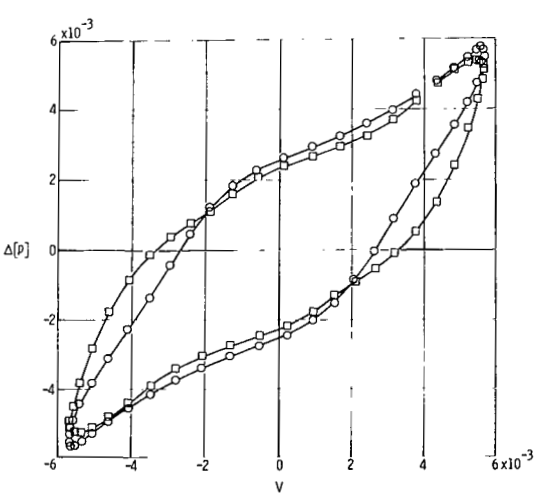

(f) Pressure - velocity trajectory. SPL = 149 db.

Figure 11.- Velocities and pressure differentials. f = 4000 Hz.

The tests at 2000 Hz (fig. 10) have the most distortion of the velocity and pressure differential signals due to higher odd harmonics. This distortion is not noticeable in the low-intensity test, but is quite marked in the high-intensity data. No subjective judgment will be given as to the agreement between the measured and computed pressure differentials shown in figures 10(e) and 10(f). Part of the discrepancies are due to nonlinear reactance and part are simply due to experimental error. In tests at other frequencies, the even harmonics were comparatively small, as theoretically predicted; however, since the 2000-Hz test data contained even harmonics of equal magnitude to the odd harmonics, the filtered data of figure 10 must be regarded with some skepticism.

Measured and computed pressure differentials from the tests at 4000 Hz (fig. 11) agree as well as the tests at 500 Hz and 1000 Hz. The reactive term is generally larger in the 4000-Hz test and remains positive during the entire cycle. There is an apparent "pinching" of the measured pressure differential trajectory which is caused by a decrease in reactance at higher velocities, but the intensity during this test was not high enough to form the loops which characterize negative reactance.

Resistance and Reactance Functions

Equation (8) was used to find the instantaneous resistance and reactance of the material sample at several times during the velocity cycle. Data at two different times, when the velocities are the same, are required to solve equation (8); therefore, the experiment does not actually measure instantaneous resistance and reactance. Since these effects are additive, it is impossible to measure them directly. Figure 12 shows the points which were used in these computations. Since the relative error in the resistance computation will be small when the velocity is large, four points where the velocity is above 1/2 the maximum velocity during each test were used for resistance computations. Four points per test were used for reactance computation also; however, these points were chosen from periods where the acceleration was comparatively large.

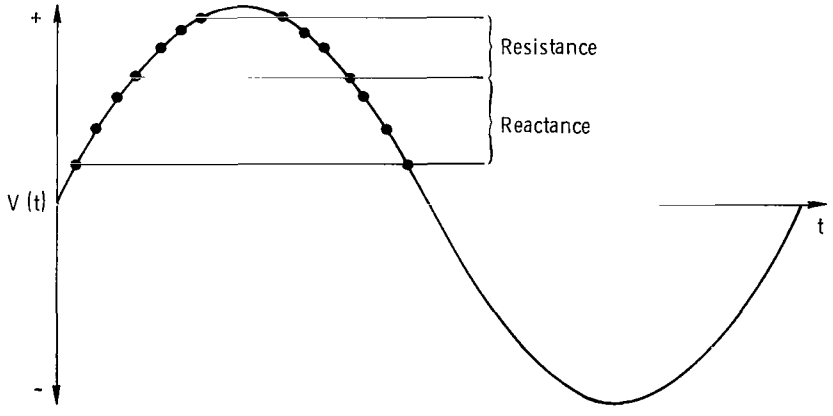

Figure 12. - Points used for resistance and reactance computations.

The resistance data from tests at different fundamental frequencies are given in figure 13. Various intensity tests were used to obtain data in the range of velocities of 10^{-4} to 10^{-2}. These data show that the instantaneous nonlinear resistance is a function of velocity only. The resistance does not depend on the fundamental frequency of the dynamic test; therefore, it must be identical to the flow resistance.

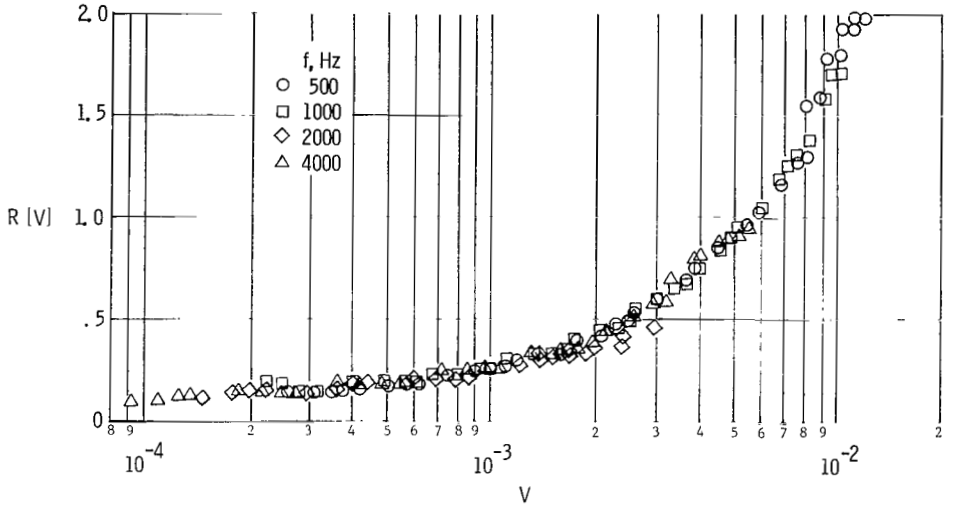

Figure 13. - Acoustically measured resistance function.

The instantaneous resistance may depend indirectly on frequency, through the velocity. If a porous material is used in a practical acoustic duct liner where there are resonant cavities behind the material, the velocity through the material will depend on the total liner impedance, which is frequency-dependent.

A single curve which approximates the instantaneous acoustic-resistance data is compared with the flow-resistance curve in figure 14. Although these functions are not

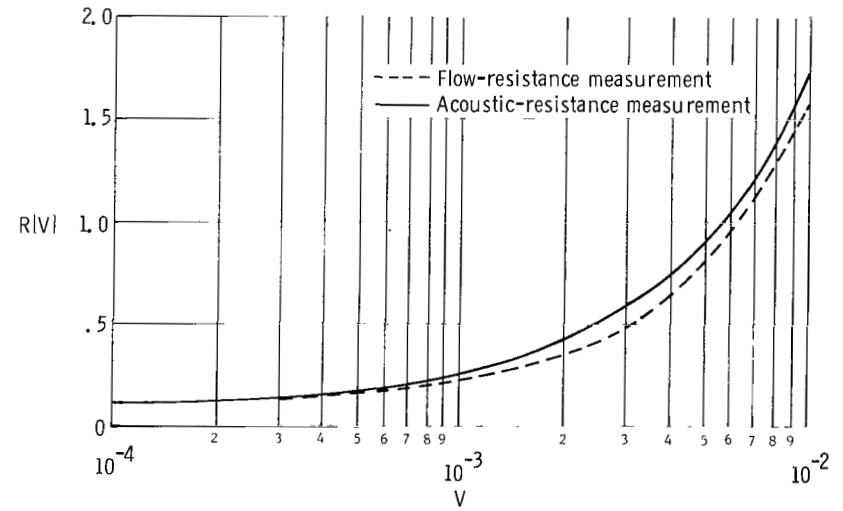

Figure 14. - Comparison of acoustic and steady measurement of resistance function.

identical, their maximum difference is 0.1, which could be due to experimental error. For most purposes, an accuracy of ±0.1 in resistance is acceptable; therefore, the flow-resistance test may be used in place of a dynamic test to find the instantaneous nonlinear resistance.

The instantaneous nonlinear reactance data are shown in figure 15. It was necessary to use frequency as a parameter to collapse these data so that they could be represented by a single function. These data show that equation (7) should be replaced by

$$\Delta\left[p(t)\right] = R\left[V(t)\right]V + \frac{f}{f_r} X\left[\frac{f_r}{f} V(t)\right] \frac{\partial V(t)}{\partial t} \tag{26}$$

where f_r is the fundamental frequency used in finding the reactance function $X\left[V\right]$ and f is the fundamental frequency of the periodic functions $\Delta\left[p(t)\right]$ and $V(t)$. Although equation (26) adequately represents the test data in this paper, it is not a satisfactory form for an instantaneous law. A truly instantaneous law may not use frequency as a parameter, since it must apply to pulses and other transients as well as periodic waves.

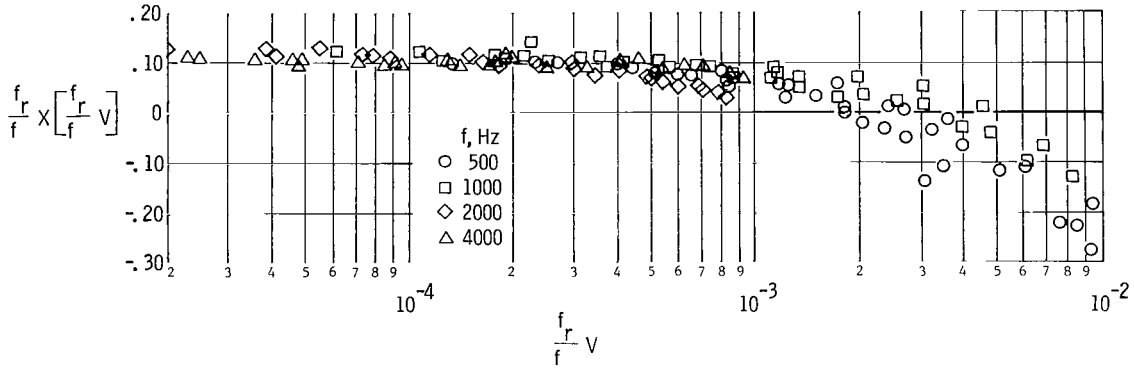

Figure 15. - Acoustically measured reactance function. f_r = 1000 Hz.

Starting from the form of equation (26), one can generalize, on the basis of dimensional analysis, to a law which would be valid for any type of excitation. A law which is generally applicable may be written in terms of dimensional variables as

$$\Delta\left[p(t)\right] = R\left[V(t)\right]V + \left(\frac{\delta}{c\tau}\right) X\left[\left(\frac{c\tau}{l}\right)\left(\frac{V}{c}\right)\right] \frac{\partial V}{\partial(t/\tau)} \tag{27}$$

where δ and l are characteristic lengths and τ is a characteristic time. The ratios (c/l) and (c/δ) have the dimensions of the reference frequency in equation (26) and the time τ is the reciprocal of a frequency f so that equation (27) is equivalent to equation (26). For transients, τ might be a rise time or a pulse duration. The argument of the reactance function X may be written as a single dimensionless group $\left(\tau \frac{V}{l}\right)$.

Although the characteristic time appears to be connected with the properties of the wave, the lengths δ and l are of uncertain origin. The length δ probably represents material thickness and l might be connected to fiber or pore size; however, more specimens must be tested to verify these possibilities.

Figure 16 compares the nonlinear reactance function to the constant reactance which was used to compute the pressure differentials presented in figures 8 to 11. The reactance will tend to become nearly constant (independent of velocity) for sufficiently high

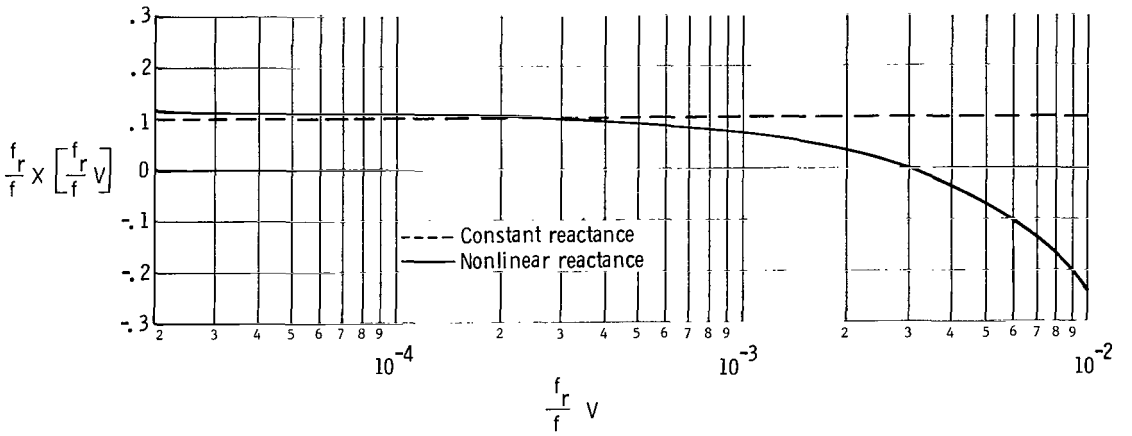

Figure 16.- Comparison of reactance function to reactance constant. f_r = 1000 Hz.

frequencies; however, for lower frequencies the reactance will depend strongly on velocity and will become negative for sufficiently large velocities. This explains the appearance of loops on the pressure-velocity trajectories from low-frequency tests. These loops were not present in the high-frequency tests.

These tests have shown that the instantaneous nonlinear resistance function may be obtained from a steady flow test. The reactance function must be found by a dynamic test. Tests at low frequencies and high intensities may be used to define the reactance function for large values of its argument, and tests at high frequencies and low intensities will define the reactance for small values of its argument. The effective intensity range of an impedance tube may be extended considerably by using tests at lower frequencies. A test at 125 Hz and 140 dB is roughly equivalent to a test at 4000 Hz and 170 dB, as far as the reactance function is concerned.

CONCLUDING REMARKS

The acoustic characteristics of a rigid porous material are given by two instantaneous relations between the acoustic velocity and pressure. The first relation is that the acoustic velocity is continuous through the material. The second relation is that the instantaneous acoustic pressure differential is given by a nonlinear operation on the

acoustic velocity. The nonlinear operator has been defined as the temporal impedance and contains two functions – the resistance and reactance functions – both of which depend on the acoustic velocity through the material. For sufficiently small velocities, both functions approach constants. These constants are the low-intensity spectral resistance and reactance.

The new theory is invariant with respect to the form of the wave. It is valid for distorted as well as nearly simple harmonic waves and may be used to account for high-intensity coupling between waves with different fundamental frequencies.

A new experimental method has been given for measuring the nonlinear temporal impedance. The method is theoretically invariant with respect to distortion of the wave; however, the data tend to scatter when distorted waves occur in the experiment. The resistance function may be measured in a steady-flow test. Acoustic tests, using the new measurement method, are necessary to measure the reactance function. High-intensity tests at low frequencies may be used to determine the reactance function for large values of its argument. Inasmuch as temporal-reactance data from the low-frequency tests may be used at higher intensities and frequencies, the effective range of an impedance tube is extended by consideration of those properties. For example, a test at 125 Hz and 140 dB results in the same temporal-reactance data as a test of 4000 Hz and 170 dB.

Langley Research Center,
National Aeronautics and Space Administration,
Hampton, Va., May 1, 1971.

REFERENCES

1. Sivian, L. J.: Acoustic Impedance of Small Orifices. J. Acoust. Soc. Amer., vol. 7, no. 2, pt. I, Oct. 1935, pp. 94-101.

2. Bolt, R. H.; Labate, S.; and Ingård, U.: The Acoustic Reactance of Small Circular Orifices. J. Acoust. Soc. Amer., vol. 21, no. 2, Mar. 1949, pp. 94-97.

3. Ingard, Uno: On the Theory and Design of Acoustic Resonators. J. Acoust. Soc. Amer., vol. 25, no. 6, Nov. 1953, pp. 1037-1061.

4. Bies, David A.; and Wilson, O. B., Jr.: Acoustic Impedance of a Helmholtz Resonator at Very High Amplitude. J. Acoust. Soc. Amer., vol. 29, no. 6, June 1957, pp. 711-714.

5. Thurston, George B.; Hargrove, Logan E., Jr.; and Cook, Bill D.: Nonlinear Properties of Circular Orifices. J. Acoust. Soc. Amer., vol. 29, no. 9, Sept. 1957, pp. 992-1001.

6. Ingard, Uno; and Ising, Hartmut: Acoustic Nonlinearity of an Orifice. J. Acoust. Soc. Amer., vol. 42, no. 1, July 1967, pp. 6-17.

7. Zorumski, William E.; and Parrott, Tony L.: Nonlinear Acoustic Theory for Thin Porous Sheets. Progress of NASA Research Relating to Noise Alleviation of Large Subsonic Jet Aircraft, NASA SP-189, 1968, pp. 17-27.

8. Zorumski, William Edward: Acoustic Scattering by a Porous Elliptic Cylinder With Nonlinear Resistance. Ph. D. Thesis, Virginia Poltech. Inst., Mar. 1970.

9. Stokes, George M.; Davis, Don D., Jr.; and Sellers, Thomas B.: An Experimental Study of Porosity Characteristics of Perforated Materials in Normal and Parallel Flow. NACA TN 3805, 1954. (Supersedes NACA RM L53H07.)

10. Pinker, R. A.; and Herbert, M. V.: The Pressure Loss Associated With Compressible Flow Through Square-Mesh Wire Gauzes. N.G.T.E. R.281, Brit. Min. Aviat., June 1966.

11. Anon.: Standard Method of Test for Impedance and Absorption of Acoustical Materials by the Tube Method. ASTM Designation: C 384-58. Pt. 14 of 1970 Annual Book of ASTM Standards. Amer. Soc. Testing Mater., 1970, pp. 126-138.

NASA-Langley, 1971 —— 23 L-7327

01U 001 48 51 3DS 71166 00903
AIR FORCE WEAPONS LABORATORY /WLOL/
KIRTLAND AFB, NEW MEXICO 87117

ATT E. LOU BOWMAN, CHIEF,TECH. LIBRARY

"The aeronautical and space activities of the United States shall be conducted so as to contribute . . . to the expansion of human knowledge of phenomena in the atmosphere and space. The Administration shall provide for the widest practicable and appropriate dissemination of information concerning its activities and the results thereof."

—NATIONAL AERONAUTICS AND SPACE ACT OF 1958

NASA SCIENTIFIC AND TECHNICAL PUBLICATIONS

TECHNICAL REPORTS: Scientific and technical information considered important, complete, and a lasting contribution to existing knowledge.

TECHNICAL NOTES: Information less broad in scope but nevertheless of importance as a contribution to existing knowledge.

TECHNICAL MEMORANDUMS: Information receiving limited distribution because of preliminary data, security classification, or other reasons.

CONTRACTOR REPORTS: Scientific and technical information generated under a NASA contract or grant and considered an important contribution to existing knowledge.

TECHNICAL TRANSLATIONS: Information published in a foreign language considered to merit NASA distribution in English.

SPECIAL PUBLICATIONS: Information derived from or of value to NASA activities. Publications include conference proceedings, monographs, data compilations, handbooks, sourcebooks, and special bibliographies.

TECHNOLOGY UTILIZATION PUBLICATIONS: Information on technology used by NASA that may be of particular interest in commercial and other non-aerospace applications. Publications include Tech Briefs, Technology Utilization Reports and Technology Surveys.

Details on the availability of these publications may be obtained from:

SCIENTIFIC AND TECHNICAL INFORMATION OFFICE

NATIONAL AERONAUTICS AND SPACE ADMINISTRATION

Washington, D.C. 20546